

Research Article

Synthesis and Evaluation of ^{18}F -Labeled Peptide for Gonadotropin-Releasing Hormone Receptor Imaging

Shun Huang, Hongsheng Li, Yanjiang Han, Lilan Fu, Yunyan Ren, Yin Zhang, Youcai Li, Penghui Sun, Meng Wang, Hubing Wu , Quanshi Wang , and Kongzhen Hu 

Nanfang PET Center, Nanfang Hospital, Southern Medical University, 1838 Guangzhou Avenue North, Guangzhou, Guangdong 510515, China

Correspondence should be addressed to Kongzhen Hu; stonglass@163.com

Received 28 November 2018; Revised 23 January 2019; Accepted 29 January 2019; Published 7 March 2019

Academic Editor: Reza Vali

Copyright © 2019 Shun Huang et al. This is an open access article distributed under the Creative Commons Attribution License, which permits unrestricted use, distribution, and reproduction in any medium, provided the original work is properly cited.

The gonadotropin-releasing hormone (GnRH) receptor is overexpressed in the majority of tumors of the human reproductive system. The purpose of this study was to develop an ^{18}F -labeled peptide for tumor GnRH receptor imaging. In this study, the GnRH (pGlu¹-His²-Trp³-Ser⁴-Tyr⁵-Gly⁶-Leu⁷-Arg⁸-Pro⁹-Gly¹⁰-NH₂) peptide analogues FP-D-Lys⁶-GnRH (FP = 2-fluoropropanoyl) and NOTA-P-D-Lys⁶-GnRH (P = ethylene glycol) were designed and synthesized. The IC₅₀ values of FP-D-Lys⁶-GnRH and NOTA-P-D-Lys⁶-GnRH were 2.0 nM and 56.2 nM, respectively. 4-Nitrophenyl-2-[^{18}F]fluoropropionate was conjugated to the ϵ -amino group of the D-lysine side chain of D-Lys⁶-GnRH to yield the new tracer [^{18}F]FP-D-Lys⁶-GnRH with a decay-corrected yield of $8 \pm 3\%$ and a specific activity of 20–100 GBq/ μmol ($n = 6$). Cell uptake studies of [^{18}F]FP-D-Lys⁶-GnRH in GnRH receptor-positive PC-3 cells and GnRH receptor-negative CHO-K1 cells indicated receptor-specific accumulation. Biodistribution and PET studies in nude mice bearing PC-3 xenografted tumors showed that [^{18}F]FP-D-Lys⁶-GnRH was localized in tumors with a higher uptake than in surrounding muscle and heart tissues. Furthermore, the metabolic stability of [^{18}F]FP-D-Lys⁶-GnRH was determined in mouse blood and PC-3 tumor homogenates at 1 h after tracer injection. The presented results indicated a potential of the novel tracer [^{18}F]FP-D-Lys⁶-GnRH for tumor GnRH receptor imaging.

1. Introduction

Gonadotropin-releasing hormone (GnRH), also known as luteinizing hormone-releasing hormone (LHRH), is a hormonal decapeptide (pGlu-His-Trp-Ser-Tyr-Gly-Leu-Arg-Pro-Gly-NH₂) produced by the hypothalamus [1]. It plays an important role in the control of mammalian reproduction. Furthermore, GnRH may have a role as a modulator of cell growth and metastasis in a number of human malignant tumors, including cancers of the breast, ovary, endometrium, and prostate [2]. GnRH activity is mediated by a specific transmembrane GnRH receptor that belongs to the G-protein-coupled receptor (GPCR) family [3–5]. The GnRH receptor is overexpressed in malignant tumors, including cancers of the breast, ovary, endometrium, prostate, larynx, melanomas, kidney, brain, and pancreas [2, 6]. In contrast to the expression in tumor cells, the GnRH receptor is expressed only at low levels in cells of healthy organs, including the

prostate, testes, and ovary, but is not present on most normal tissues [6–9]. This indicates a broad connection between cancerous transformation and GnRH receptor expression. Therefore, noninvasive imaging of the expression of the GnRH receptor would be of great help for the early detection of cancer, the evaluation of tumor progression, and monitoring of cancer treatment efficacy.

Advancement in imaging techniques such as positron-emission tomography (PET) can monitor in vivo molecular events noninvasively and provide functional information on diseases [10]. Over the past two decades, several studies reported the development of radiolabeled GnRH peptides for targeting GnRH receptors [11–18], but only a few have been successfully imaged by PET or SPECT [15–18]. In 2010, Jalilian et al. reported that [^{111}In]-DTPA-buserelin was prepared for GnRH receptor studies but was only imaged and evaluated in normal rat with SPECT [15]. The next year, Guo et al. reported the design and synthesis of

^{111}In -DOTAAhx-(D-Lys⁶-GnRH1) as a potential SPECT probe for breast cancer imaging [16]. In 2017, Xu et al. reported a similar SPECT probe ^{111}In -DOTA-Aoc-D-Phe-(D-Lys⁶-GnRH) and imaged in DU145 human prostate cancer-xenografted nude mice [18]. GnRH peptide analogues labeled with positron-emitting radionuclides are of particular interest due to the high spatial resolution and sensitivity of PET [19]. Recently, Zoghi et al. developed [^{68}Ga]-labeled DOTA-triptorelin as a possible PET radiotracer for GnRH receptor imaging [17]. The biodistribution of the tracer was determined in normal male rats and 4T1 tumor-bearing mice. However, neither PET imaging nor the uptake data of the 4T1 tumor were reported for the tracer.

In this study, we introduce the prosthetic group of 4-nitrophenyl-2- ^{18}F fluoropropionate (^{18}F NFP) to the ϵ -amino group of the D-lysine side chain of D-Lys⁶-GnRH (pGlu¹-His²-Trp³-Ser⁴-Tyr⁵-D-Lys⁶-Leu⁷-Arg⁸-Pro⁹-Gly¹⁰-NH₂), which has demonstrated higher binding affinity and stability than native GnRH [20, 21]. The resulting probe, ^{18}F FP-D-Lys⁶-GnRH, was evaluated in a PC-3 human prostate cancer-xenografted model using micro-PET imaging. Extensive *in vitro*, *ex vivo*, and *in vivo* experiments were performed to evaluate its usefulness and pharmacokinetics as a PET tracer for noninvasive imaging of GnRH receptor expression.

2. Materials and Methods

2.1. General. All commercially available materials were used without further purification. The D-Lys⁶-GnRH [(Glp)-HWSY(D)KLRPG-NH₂], [His⁵, D-Tyr⁶]GnRH [(Glp)-HWSH(D)YLRPG-NH₂], and NOTA-P-D-Lys⁶-GnRH (P = PEG₃) were custom manufactured from GL Biochem Ltd. (Shanghai, China). Sep-Pak light QMA and Plus C18 cartridges were obtained from Waters Corporation (Milford, MA, USA). High-performance liquid chromatography (HPLC) separation was performed on the PET-MF-2V-IT-I synthesizer module (PET Co. Ltd., Beijing, China) built-in HPLC system with a semipreparative reverse-phase C18 column (10 × 250 mm). Analytical HPLC was performed using a LC-20AD HPLC system (Shimadzu, Japan) equipped with a ZORBAX Eclipse XDB-C18 analytic column (4.6 × 150 mm, 5 μm ; Agilent Technologies, USA). Radioactivity was measured by a calibrated ion chamber (Capintec CRC-15R, Capintec, Inc. NJ, USA) or a gamma counter (γ -counter) (CAPRAC-R, Capintec, Inc. NJ, USA). High-resolution mass spectra were recorded with a Thermo Fisher Scientific Orbitrap Fusion mass spectrometer. No-carrier-added ^{18}F -fluoride was obtained by reacting $^{18}\text{O}(p, n)^{18}\text{F}$ in a GE PET trace cyclotron with irradiating enriched [^{18}O]water (98%). Statistical analysis was performed using Microsoft Office Excel. Continuous variables were analyzed using the Student's *t*-test with a significance level of *P* value less than 0.05.

2.2. Synthesis of NFP. The synthesis of NFP was performed as described previously [22]. In brief, to a solution of 2-fluoropropionic acid (75 mg, 0.82 mmol) in dry DMSO (1 mL) diisopropylethylamine (DIPEA, 100 μL) and Bis(4-nitrophenyl) carbonate (259 mg, 0.82 mmol) were added at

room temperature. The reaction mixture was stirred at 60°C for 3 h and was then cooled to room temperature and quenched with 5% acetic acid solution (1 mL). The product was purified by flash chromatography on silica gel (EtOAc:hexanes = 1:1) to yield the title compound as a red solid (61 mg, 0.54 mmol, 66% yield). NMR spectroscopy: ^1H NMR (400 MHz, CDCl_3) δ 8.30 (d, J = 8.8 Hz, 2H), 7.36 (d, J = 8.8 Hz, 2H), 5.30 (dd, J = 48.1, 6.9 Hz, 1H), and 1.77 (dd, J = 23.4, 6.9 Hz, 3H). ^{13}C NMR (100 MHz, $(\text{CD}_3)_2\text{SO}$, 25°C, δ): 168.1 (d, J = 24 Hz), 154.6, 145.8, 125.3, 122.3, 85.4 (d, J = 183 Hz), and 18.3 (d, J = 22 Hz).

2.3. Synthesis of FP-D-Lys⁶-GnRH. NFP-labeled D-Lys⁶-GnRH was prepared according to a published procedure with modifications [22]. In brief, to a solution of D-Lys⁶-GnRH (5 mg, 4.0 μmol in 0.2 mL of DMSO and 40 μL of DIPEA), NFP (0.85 mg, 4.0 μmol in 0.1 mL of DMSO) was slowly added at room temperature. The reaction mixture was stirred at room temperature for 3 h. The desired product was purified by semipreparative HPLC and lyophilized to yield FP-D-Lys⁶-GnRH as a white powder (3.2 mg, 2.4 μmol , 60% yield). Analytical HPLC (R_t = 13.9 min) and HRMS (*m/z*: calculated for $\text{C}_{62}\text{H}_{87}\text{FN}_{18}\text{O}_{14}$ ($[\text{M} + 2\text{H}]^{2+}$), 664.3383; found, 664.3389) analyses confirmed the product identification.

2.4. Radiosynthesis of [^{131}I](His⁵, D-Tyr⁶)GnRH. [^{131}I](His⁵, D-Tyr⁶)GnRH was prepared according to a similar published procedure [11, 14]. (His⁵, D-Tyr⁶)GnRH (100 μg) in 100 μL of Tris-HCl (25 mM, 0.4 M NaCl, PH 7.5) was reacted with Na^{131}I (37 MBq; HTA CO. LTD. China), NaOH (10 μL , 0.05 M), and chloramine-T (50 μL , 1 mg/mL) for 30 min at room temperature. The reaction was terminated by the addition of $\text{Na}_2\text{S}_2\text{O}_5$ solution (10 μL , 1 mg/mL). Iodinated peptide was purified by HPLC with a gradient of 95% solvent A and 5% solvent B (0–2 min) ramped to 50% solvent A and 50% solvent B at 50 min.

2.5. In Vitro Receptor Binding Assay. GnRH membrane preparations were obtained from Millipore ChemiScreen (HTS027M). The GnRH receptor binding affinities (IC_{50} values) of FP-D-Lys⁶-GnRH, D-Lys⁶-GnRH, and NOTA-P-D-Lys⁶-GnRH were determined by *in vitro* competitive binding assay according to the manufacturer's protocol. In brief, 5 μL of Millipore ChemiScreen human GnRH membrane preparations was incubated at room temperature for 1.5 h with approximately 20,000 counts per minute (cpm) of [^{131}I](His⁵, D-Tyr⁶)GnRH in the presence of 10^{-11} to 10^{-5} M of each peptide in 95 μL of binding buffer (50 mM HEPES, 5 mM MgCl_2 , 1 mM CaCl_2 , 0.2% BSA, buffer to pH 7.4 using 1 M NaOH). After the incubation, 600 μL of ice-cold washing buffer (50 mM HEPES, 500 mM NaCl, 0.1% BSA, buffer to pH 7.4 using 1 M NaOH) was added to each mixture. Each resulting mixture was filtered through a GF/C filter (Whatman, Clifton, NJ) presoaked in 0.33% polyethylenimine. Each filter was rinsed with 1 mL of ice-cold wash buffer six times. The activities on the filters were measured in a gamma counter (γ -counter).

2.6. Radiosynthesis of [^{18}F]FP-D-Lys 6 -GnRH. [^{18}F]NFP was prepared and used for peptide radiolabeling based on a previously reported procedure [23]. In brief, a solution of D-Lys 6 -GnRH (50 μg) in DMSO (200 μL) and DIPEA (40 μL) was added to anhydrous [^{18}F]NFP. The reaction mixture was stirred for 10 min at 40°C and was diluted with water (10 mL). The dilution was passed through a Plus C18 cartridge, and then the cartridge was washed with water (10 mL). The desired radiolabeled compound was eluted with 2 mL of ethanol. For in vitro and in vivo experiments, the solvent was evaporated in vacuo and [^{18}F]FP-D-Lys 6 -GnRH was formulated with 0.9% saline.

2.7. Octanol/Water Partition Coefficient. Approximately 740 KBq of [^{18}F]FP-D-Lys 6 -GnRH was added to a vial containing 5 mL each of *n*-octanol and phosphate-buffered saline (PBS) (pH = 7.4). The mixture was vigorously vortexed for 1 min and centrifuged for 4 min to ensure the complete separation of layers. After centrifugation, three hundred milliliters of each layer were measured using a γ -counter, and logP values were calculated ($n = 3$).

2.8. In Vitro Stability. An aliquot of [^{18}F]FP-D-Lys 6 -GnRH (2.22 MBq, 10 μL) in normal saline was added to PBS (200 μL) or bovine serum (200 μL) and incubated at 37°C for 2 h. For the PBS study, an aliquot of the solution was directly injected into a radio-HPLC for analysis. The bovine serum sample was filtered through a 0.22- μm Millipore filter and injected into a radio-HPLC column for analysis.

2.9. Metabolic Stability. The metabolic stability of [^{18}F]FP-D-Lys 6 -GnRH was evaluated in tumor-bearing nude mice according to a published procedure [24] with some modifications. Approximately 10 MBq of [^{18}F]FP-D-Lys 6 -GnRH was injected intravenously in a conscious nude mouse bearing a PC-3 tumor as the control group ($n = 2$ per group). For the blocking experiment, the tumor-bearing mice were coinjected with 15 mg/kg mouse body weight of D-Lys 6 -GnRH and 10 MBq of [^{18}F]FP-D-Lys 6 -GnRH ($n = 2$ per group). The mice were sacrificed at 1 h after injection, blood was obtained retro-orbitally, and the tumors were removed. The blood was then centrifuged (12000 g, 10 min). Tumors were separately homogenized in 0.5 mL of ethanol and centrifuged (12000 g, 10 min). The supernatant was filtered through a 30 KD Millipore filter and analyzed by HPLC. HPLC samples were collected in 0.5 min fractions for 30 min. The samples were counted in a γ -counter for 20 s. The counts were decay corrected to the injection time and added together. The counts were as the plotted intensity (cpm) versus fractions to show the profile of the sample. The data were plotted to reconstruct the HPLC spectrum.

2.10. Cell Culture and Animal Models. PC-3 human prostate cancer, SKBR-3 breast tumor, and CHO-K1 cell lines were purchased from the Institute of Biochemistry and Cell Biology, Shanghai Institutes for Biological Sciences, Chinese Academy of Sciences (Shanghai, China). Tumor cells

($2\text{--}5 \times 10^6$) were injected subcutaneously and allowed to grow for 2 to 4 weeks. At the time of the experiments, the tumor reached 3–6 mm (diameter), and the mice were 6–8 weeks old and weighed 16–24 g. All studies were approved by the Nanfang Hospital Animal Ethics Committee at the Southern Medical University.

2.11. Cell Uptake. PC-3 and CHO-K1 cells were seeded into 12-well plates at a density of 5×10^5 cells/well and incubated overnight. In the cell uptake experiment, PC-3 and CHO-K1 cells were washed thrice with PBS, and then [^{18}F]FP-D-Lys 6 -GnRH or with 10 μM D-Lys 6 -GnRH was added in quadruplicate (1.3 μCi /well). After incubation at 37°C for 30 min, cells were rinsed thrice with PBS and lysed with NaOH-SDS (sodium dodecyl sulfate) (0.2 M NaOH, 1% SDS). The cell lysate was collected and measured in a γ -counter.

2.12. Micro-PET Studies. Dynamic micro-PET studies with tumor-bearing mice were performed using the Inveon MicroPET/CT scanner. A total of 5.55–7.4 MBq of [^{18}F]FP-D-Lys 6 -GnRH was injected intravenously into animals via the tail vein. For the blocking experiment, the tumor-bearing mice were coinjected with 15 mg/kg mouse body weight of D-Lys 6 -GnRH and [^{18}F]FP-D-Lys 6 -GnRH ($n = 3$ per group). Dynamic scans were conducted over a period of 2 h. PET images were reconstructed using a three-dimensional ordered-subset expectation maximum algorithm. For data analysis, the region of interests (ROIs) were manually drawn over the tumor and major organs on decay-corrected whole-body coronal images using vendor software.

2.13. In Vivo Biodistribution. The PC-3 xenograft-bearing nude mice ($n = 4$ for each group) were injected with approximately 1.0 MBq of [^{18}F]FP-D-Lys 6 -GnRH via the tail vein. Animals were sacrificed at 120 min postinjection. The tumor and the other tissue samples of interest were rapidly dissected and weighed. ^{18}F radioactivity was counted with a γ -counter. The results were calculated as the percentage injected dose per gram tissue or organ (% ID/g) ($n = 4$).

2.14. Immunohistochemistry. The immunohistochemistry staining was performed on PC-3 and SKBR-3 cancer-xenografted tumors to demonstrate the GnRH receptor expression. The immunoperoxidase staining of the xenografted tumor slices (4 μm thickness) were performed according to the protocol for the envision horseradish peroxidase system (DAKO EnVision System K5007) following the manufacturer's protocol. The primary antibody used in this study was GnRH receptor (Abcam ab183079, 1:50). Negative (no primary antibody) controls were included in the staining experiment. The cytoplasmic staining of the GnRH receptor was recorded as negative, weak, moderate, and strong [25].

3. Results

3.1. Chemistry. Nonradioactive FP-D-Lys 6 -GnRH was used as a reference standard for radiosynthesis and for receptor binding assays. FP-D-Lys 6 -GnRH was prepared by direct

conjugation of NFP to D-Lys⁶-GnRH peptide with a yield of 52%. The product was purified by semipreparative RP-HPLC to achieve greater than 95% purity, and the correct molecular masses were confirmed by using orbitrap fusion mass spectrometry.

3.2. In Vitro Receptor Binding Assay. The GnRH receptor affinities for FP-D-Lys⁶-GnRH, D-Lys⁶-GnRH, and NOTA-P-D-Lys⁶-GnRH were determined using human GnRH membrane preparations and [¹³¹I](His⁵, D-Tyr⁶)GnRH as the radioligand. The IC₅₀ values of FP-D-Lys⁶-GnRH, D-Lys⁶-GnRH, and NOTA-P-D-Lys⁶-GnRH were 2.0 nM, 15.8 nM, and 56.2 nM, respectively ($n = 3$) (Figure 1). Since FP-D-Lys⁶-GnRH showed the strongest GnRH receptor binding affinity, we further evaluated [¹⁸F]FP-D-Lys⁶-GnRH.

3.3. Radiochemistry. For the radiosynthesis of [¹⁸F]FP-D-Lys⁶-GnRH, we followed our previously published four-step two-pot methodology [23]. After ¹⁸F-fluorination of the bromo precursor and its hydrolysis with KOH, the 2-[¹⁸F] fluoropropanoate salt was activated with bis(4-nitrophenyl) carbonate to yield the [¹⁸F]NFP. Using 40 nmol of D-Lys⁶-GnRH was coupled to [¹⁸F]NFP at 40°C for 10 min (Figure 2). The product, [¹⁸F]FP-D-Lys⁶-GnRH, was isolated by solid-phase extraction without the need for HPLC separation with an overall yield of $8 \pm 3\%$ (decay corrected, referred to [¹⁸F]fluoride) and high specific activities of 20–100 GBq/ μ mol ($n = 6$).

3.4. Octanol/Water Partition Coefficient. The lipophilicity of [¹⁸F]FP-D-Lys⁶-GnRH was determined using the *n*-octanol/PBS distribution method. The logP_{7.4} value for the [¹⁸F]FP-D-Lys⁶-GnRH was -2.13 ± 0.04 ($n = 3$).

3.5. In Vitro Stability and In Vivo Metabolism. To complete the determination of the in vitro characteristics of [¹⁸F]FP-D-Lys⁶-GnRH, the stability was determined by incubation of the radiotracer in PBS and bovine serum at 37°C for 2 h. [¹⁸F]FP-D-Lys⁶-GnRH showed high stability for up to 120 min, as determined by radio-HPLC analysis, and the unchanged tracer was greater than 95% (Figure 3(a)). Metabolites of [¹⁸F]FP-D-Lys⁶-GnRH in vivo after 1 h were analyzed in the PC-3 tumor-bearing mouse (Figure 3(b)). The results are summarized in Table 1. The extraction efficiency of tumor and blood was between 67% and 72% in both control and blocking groups (Table 1). In the control group, $23 \pm 1.2\%$ and $33 \pm 0.10\%$ of radioactivity were unchanged tracer in the supernatant of blood and tumor, respectively. Blockade of GnRH receptors with D-Lys⁶-GnRH resulted in an increment in unchanged tracer proportion by $41 \pm 6.7\%$ and $43 \pm 2.2\%$ in the supernatant of blood and tumor, respectively.

3.6. Cell Uptake. The cell uptake of [¹⁸F]FP-D-Lys⁶-GnRH was evaluated in PC-3 human prostate GnRH receptor-positive cells and GnRH receptor-negative cells, CHO-K1. The results are shown in Figure 4. PC-3 cells express a high

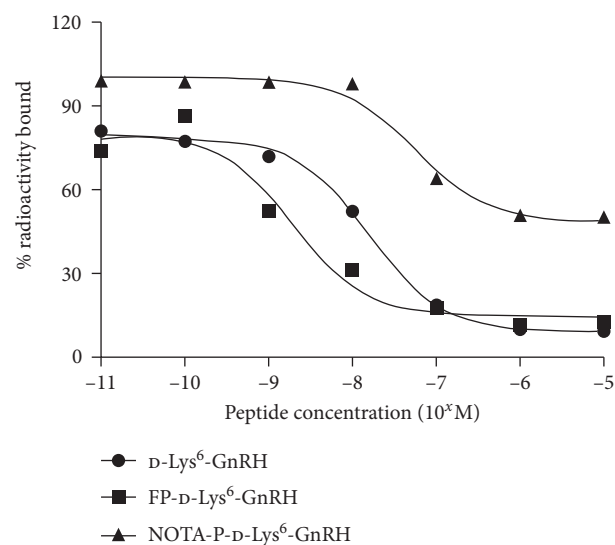


FIGURE 1: The competitive binding curves of D-Lys⁶-GnRH, FP-D-Lys⁶-GnRH, and NOTA-P-D-Lys⁶-GnRH. Data represent one of three separate experiments.

level of GnRH [26], and the uptake of [¹⁸F]FP-D-Lys⁶-GnRH is rapid and high, reaching approximately 4% within 30 min of incubation. By contrast, due to the relatively low GnRH receptor density of CHO-K1 cells [27], [¹⁸F]FP-D-Lys⁶-GnRH had relatively low cell uptake (<0.3%). Incubation of 10 μ M of D-Lys⁶-GnRH peptide blocked the PC-3 cells uptake (<0.3%), indicating that the binding of [¹⁸F]FP-D-Lys⁶-GnRH was GnRH receptor-specific.

3.7. Micro-PET Imaging Studies. Dynamic micro-PET studies for nude mice bearing PC-3 and SKBR-3 tumor xenografts were performed with [¹⁸F]FP-D-Lys⁶-GnRH (Figure 5). Animal PET images of summed 60 min coronal sections were selected for visualization (Figure 5(a)). As the images demonstrate, tumors could be visualized within each animal model. [¹⁸F]FP-D-Lys⁶-GnRH had higher tumor uptake in the PC-3 prostate tumor model than the SKBR-3 breast tumor model. Furthermore, blocking experiments were performed on PC-3 tumor-bearing mice. Representative coronal images of PC-3 tumor mice at 5, 15, 30, 60, 90, and 120 min after injection of [¹⁸F]FP-D-Lys⁶-GnRH in the presence of D-Lys⁶-GnRH (15 mg/kg) are illustrated in Figure 5(b). As the images showed, the tumor uptake in the control group was faster and more clearly visible compared with the blocking group. High gall bladder, kidney, and bladder uptake was observed in the animal model. To confirm this finding, a region-of-interest (ROI) analysis was performed on the reconstructed images to generate the time-activity curves for [¹⁸F]FP-D-Lys⁶-GnRH (Figure 5(c)). For the control group of the PC-3 tumor model, rapid tumor uptake was visualized in the first 15–20 min. Maximum tumor uptake was reached within the first 20 min after injection. Tumor uptake then slowly washed out throughout the 120 min scan time, suggesting that the radioactivity was taken up and trapped in the tumor tissue. In contrast, the presence of a blocking dose of D-Lys⁶-GnRH reduced the

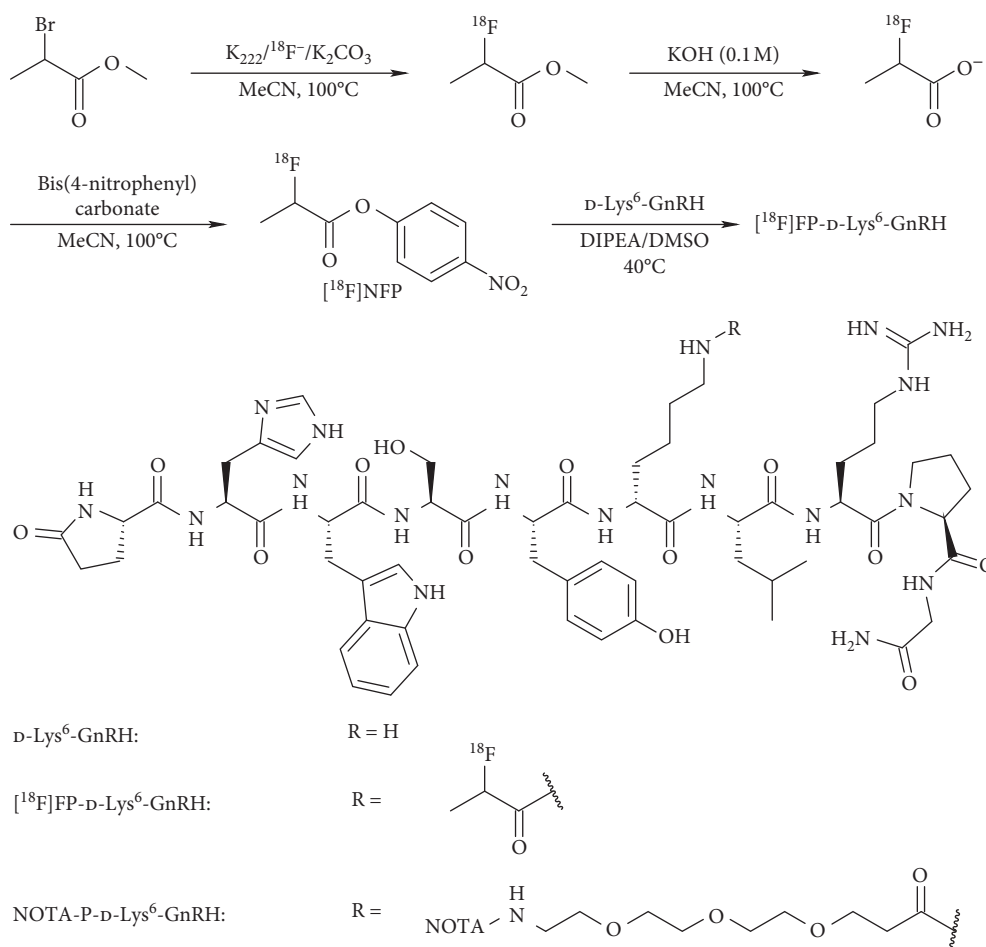


FIGURE 2: The multistep radiosynthesis of $[\text{}^{18}\text{F}]\text{FP-D-Lys}^6\text{-GnRH}$ and the structures of GnRH analogues.

tumor uptake during the first 50 min. After that, the tumor uptake was higher than the control group and remained consistent throughout the 120 min scan time, with little to no washout observed. The absolute radioactivity accumulation in the muscle and heart of the blocking group was higher than that observed in the control group. The ratios of tumor-to-muscle and tumor-to-heart in the blocking group were lower than the control group throughout the 120 min scan time (Figure 5(d)). Tumor-to-muscle and tumor-to-heart ratios were 3.55 and 2.01, respectively, at 1 h i.v. for the control group. In comparison, the ratios for tumor-to-muscle and tumor-to-heart for the blocking group were 1.14 and 0.78, respectively.

3.8. Biodistribution Studies. To validate the micro-PET imaging experiments, biodistribution studies of $[\text{}^{18}\text{F}]\text{FP-D-Lys}^6\text{-GnRH}$ were performed at 2 h after intravenous dosing in PC-3 xenograft models. The results are shown in Figure 6. No significant differences were observed compared to the micro-PET image quantification. Compared to the control group, $[\text{}^{18}\text{F}]\text{FP-D-Lys}^6\text{-GnRH}$ in the blocking group resulted in higher uptake in the organs, except the gall bladder, kidney, intestine, stomach, and spleen. These results indicate that the tracer excretes through the gall bladder system and that the metabolic rate was slow in excess $\text{D-Lys}^6\text{-GnRH}$.

Although PC-3 tumor uptake in the blocking group was higher than in the control group, the ratio of tumor-to-muscle in the control group was higher than in the blocking group (2.5 vs 1.6, $p < 0.05$).

3.9. Immunohistochemistry. The GnRH receptor expression in PC-3 prostate cancer and SKBR-3 breast tumor slices was confirmed by immunohistochemistry staining. The immunohistochemistry staining results are presented in Figure 7. The cytoplasmic staining of the GnRH receptor in PC-3 human prostate cancer was strong. In contrast, the cytoplasmic staining of GnRH receptor in SKBR-3 breast tumor was weak. Hence, we used the PC-3 and SKBR-3 tumor-bearing mice models to determine the tumor targeting and pharmacokinetic properties of $[\text{}^{18}\text{F}]\text{FP-D-Lys}^6\text{-GnRH}$.

4. Discussion

The expression of GnRH and its receptor in human malignant tumors of the urogenital tract is part of an autocrine system, which regulates cell proliferation [2]. GnRH receptor overexpression occurs in many malignancies and is a suitable target for cancer therapy [2, 3, 28–30]. As such, the in vivo imaging of GnRH receptor expression would serve as an imaging marker for tumor growth, providing critical

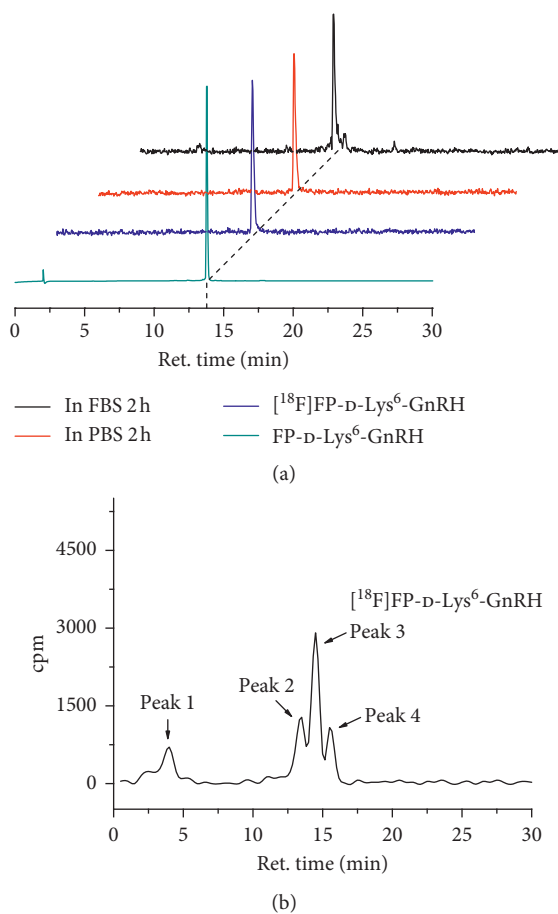


FIGURE 3: HPLC analysis the stability of $[^{18}\text{F}]\text{FP-D-Lys}^6\text{-GnRH}$: (a) $[^{18}\text{F}]\text{FP-D-Lys}^6\text{-GnRH}$ incubation in PBS and bovine serum for 2 h compared to $[^{18}\text{F}]\text{FP-D-Lys}^6\text{-GnRH}$ from the quality control and its reference standard $\text{FP-D-Lys}^6\text{-GnRH}$; (b) representative HPLC profiles displaying unchanged $[^{18}\text{F}]\text{FP-D-Lys}^6\text{-GnRH}$ (peak 3) and its metabolites (peak 1, peak 2, and peak 4) in PC-3 tumors at 1 h after intravenous injection in the blocking group. ret. = retention time in min.

TABLE 1: Proportions of supernatant and unchanged $[^{18}\text{F}]\text{FP-D-Lys}^6\text{-GnRH}$ in nude mice bearing PC-3 tumor at 1 h after intravenous injection for control and blocking groups.

	Blood	Tumor	15 mg/kg	
			Blood	Tumor
Supernatant (%)	72 ± 8.2	67 ± 15	71 ± 8.8	72 ± 18
Unchanged tracer (%)	23 ± 1.2	33 ± 0.10	41 ± 6.7	43 ± 2.2

diagnostic and prognostic information for the management of a patient with cancer.

Although a few radiolabeled peptides are being evaluated for tumor and GnRH receptor imaging [15–18], no successful PET tracer has been reported to our knowledge. The GnRH agonist $\text{D-Lys}^6\text{-GnRH}$ has served as a carrier to target chemotherapy agents or radionuclides to the GnRH receptor for cancer treatment or imaging [6, 9, 13, 14, 16, 26, 30–34]. In this study, we conjugated a small 2-fluoropropionate group to $\text{D-Lys}^6\text{-GnRH}$ ($\text{FP-D-Lys}^6\text{-GnRH}$) and NOTA to

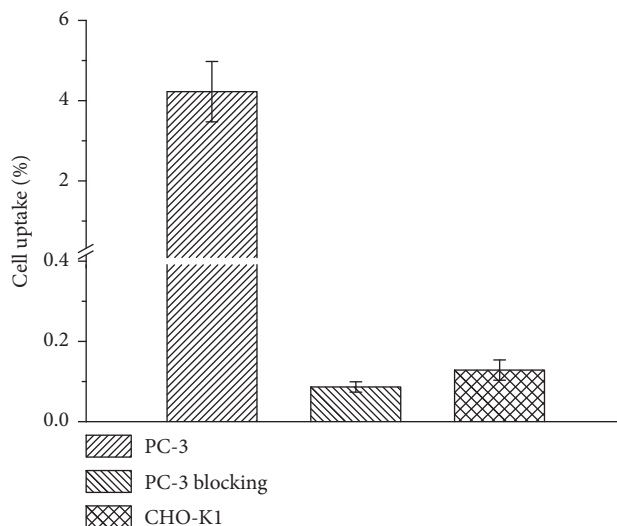


FIGURE 4: Cell uptake studies using PC-3 tumor cells (GnRH receptor-positive) and CHO-K1 cells (GnRH receptor-negative) ($n = 3$, mean ± SD). Blocking studies with $10\ \mu\text{M}$ $\text{D-Lys}^6\text{-GnRH}$ confirmed the receptor-specific uptake.

the D-Lys^6 via the PEG linker to $\text{D-Lys}^6\text{-GnRH}$ (NOTA- $\text{P-D-Lys}^6\text{-GnRH}$). Receptor binding assays using membrane preparations and $[^{131}\text{I}](\text{His}^5, \text{D-Tyr}^6)\text{GnRH}$ as the radioligand showed that $\text{FP-D-Lys}^6\text{-GnRH}$ ($\text{IC}_{50} = 2.0\ \text{nM}$) was approximately 8-fold higher in potency than the reference $\text{D-Lys}^6\text{-GnRH}$ ($\text{IC}_{50} = 15.8\ \text{nM}$). The NOTA- $\text{P-D-Lys}^6\text{-GnRH}$ ($\text{IC}_{50} = 56.2\ \text{nM}$) dramatically decreased the GnRH receptor binding affinity by approximately 4-fold. $\text{FP-D-Lys}^6\text{-GnRH}$ displayed 2.0 nM GnRH receptor binding affinity, warranting its further evaluation. We introduce ^{18}F into $\text{D-Lys}^6\text{-GnRH}$ using the prosthetic group $[^{18}\text{F}]\text{NFP}$, which as a small ^{18}F -radiolabeling group for peptides has less influence on the characteristics of peptides [22]. Furthermore, some peptides labeled with $[^{18}\text{F}]\text{NFP}$ are successfully used in clinical trials in human subjects [35]. Moreover, in cell uptake studies using GnRH receptor-positive PC-3 cells and GnRH receptor-negative CHO-K1 cells, it could be demonstrated that $[^{18}\text{F}]\text{FP-D-Lys}^6\text{-GnRH}$ was specifically binding to the GnRH receptor. The receptor-specific uptake is also confirmed by micro-PET imaging in PC-3 prostate and SKBR-3 tumor models. The GnRH receptor expression in the two model tumors was confirmed by immunohistochemistry staining.

$[^{18}\text{F}]\text{FP-D-Lys}^6\text{-GnRH}$ was evaluated in the PC-3 prostate xenograft model and showed tumor uptake and primarily gall bladder system excretion routes. Liver uptake was significant and followed by biliary tract excretion, which was observed after 2 h, consistent with other radiolabeled peptides [15]. The radioactivity has moderate accumulation in the kidney and intestine, possibly because the hydrophilic metabolites of the $[^{18}\text{F}]\text{FP-D-Lys}^6\text{-GnRH}$ were excreted through the kidneys. In the control group, $[^{18}\text{F}]\text{FP-D-Lys}^6\text{-GnRH}$ exhibited rapid tumor uptake and reached a maximum at 20 min i.v. and then was slowly washed out. However, $[^{18}\text{F}]\text{FP-D-Lys}^6\text{-GnRH}$ exhibited maximum tumor uptake at 60 min i.v., and sustained tumor accumulation was

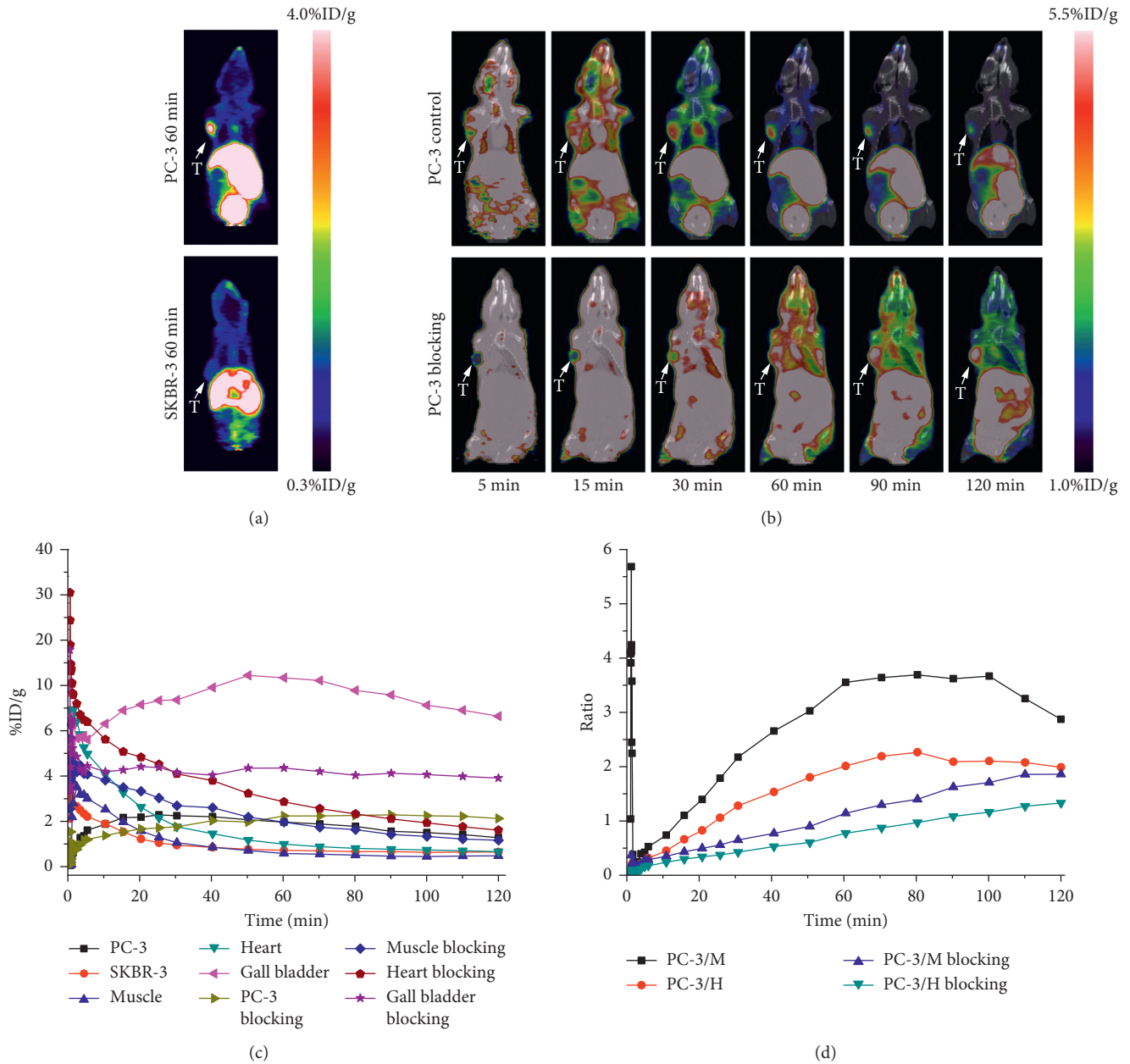


FIGURE 5: (a) Micro-PET images of $[^{18}\text{F}]\text{FP-D-Lys}^6\text{-GnRH}$ in nude mice bearing PC-3 and SKBR-3 tumors at 60 min after intravenous injection. (b) MicroPET/CT images of $[^{18}\text{F}]\text{FP-D-Lys}^6\text{-GnRH}$ in nude mice bearing the PC-3 tumor at 5, 15, 30, 60, 90, and 120 min after intravenous injection for control and blocking groups. Images are shown in coronal views. Tumors are indicated by arrowheads. (c) Time-activity curves illustrate $[^{18}\text{F}]\text{FP-D-Lys}^6\text{-GnRH}$ dynamics in selected ROIs. (d) Comparison of the tumor to muscle and heart ratios of $[^{18}\text{F}]\text{FP-D-Lys}^6\text{-GnRH}$ in nude mice bearing PC-3 tumors from 0 to 120 min after intravenous injection for control and blocking groups ($n = 3/\text{group}$). T: tumor; M: muscle; H: heart.

observed in the blocking group. Furthermore, muscle and heart uptake in the blocking group was higher than in the control group throughout the 120 min scan time, which was consistent with the literature reported for $[^{125}\text{I}]\text{triptorelin}$ [14]. In order to find the reason, the metabolic stability studies of $[^{18}\text{F}]\text{FP-D-Lys}^6\text{-GnRH}$ were performed in the PC-3 tumor-bearing mouse. The proportion of radioactivity in the supernatant from blood and tumors was not significantly different in control and blocking groups. For the proportions of the unchanged tracer in blood and tumors, the blocking

group were higher than in the control group. The results showed that excretion of the tracer was slow in the excess of $\text{D-Lys}^6\text{-GnRH}$.

Through the in vivo and in vitro studies of $[^{18}\text{F}]\text{FP-D-Lys}^6\text{-GnRH}$ developed in this study, we believe that ^{18}F -labeled GnRH peptide is a potential tracer for GnRH expression. However, high radioactivity accumulation in the gall bladder and abdomen will limit its application in detecting lesions that are in the gall bladder and around the urinary bladder. Further optimization of the scaffold to

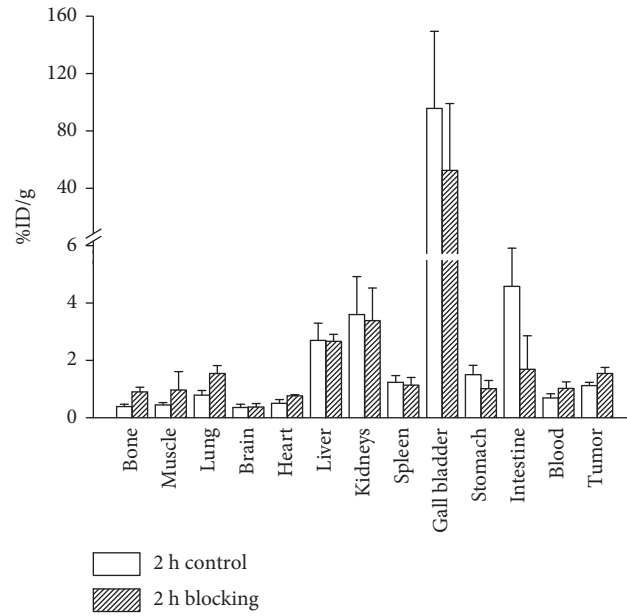


FIGURE 6: Biodistribution data of $[^{18}\text{F}]\text{FP-D-Lys}^6\text{-GnRH}$ in nude mice bearing PC-3 tumors at 1 h postinjection. All data are expressed as the mean values \pm SD ($n = 4$).

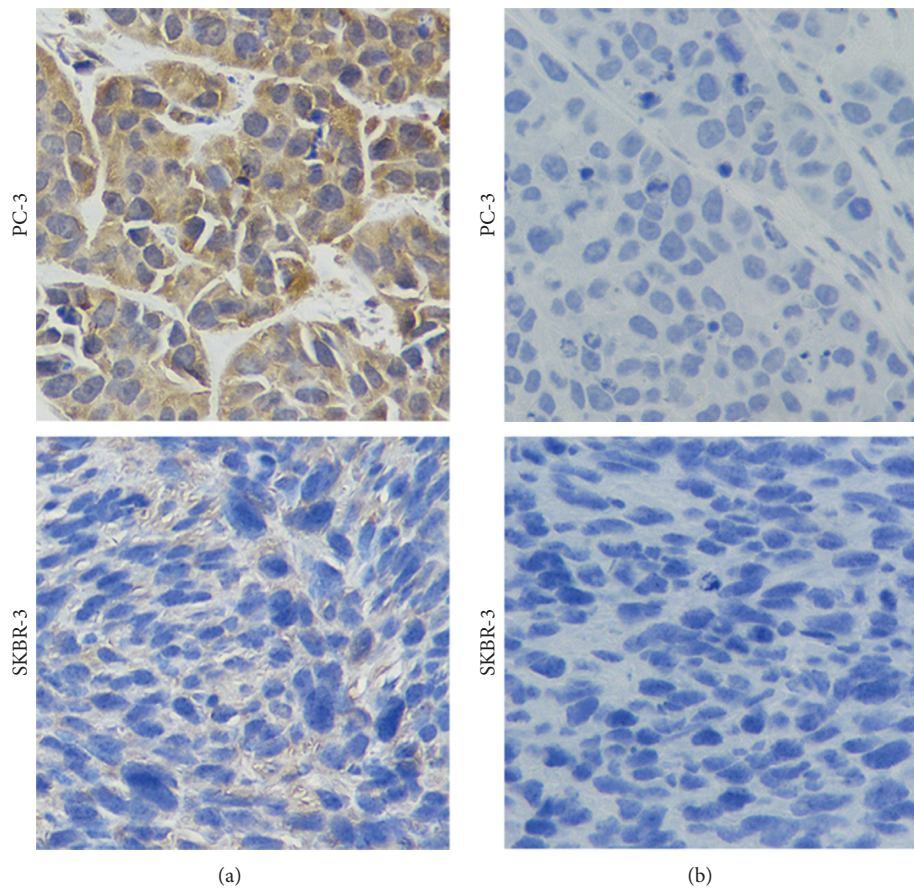


FIGURE 7: Immunohistochemical staining of GnRH receptor expression in PC-3 and SKBR-3 xenografted tumors: (a) the PC-3 xenografted tumor exhibited strong brown cytoplasmic staining and the SKBR-3 xenografted tumor exhibited weak brown cytoplasmic staining; (b) the PC-3 and SKBR-3 xenografted tumors were stained without primary goat antihuman GnRH antibody ($\times 400$).

reduce or eliminate radioactivity uptake in the abdomen is underway in our laboratories.

5. Conclusions

We successfully radiolabeled D-Lys⁶-GnRH with the small prosthetic group [¹⁸F]NFP. In vitro assays, in vivo imaging, and biodistribution studies showed that [¹⁸F]FP-D-Lys⁶-GnRH exhibited high affinity for the GnRH receptor, predominant gall bladder system elimination, and specific tumor uptake in tumor xenografts. As a result, [¹⁸F]-labeled GnRH peptide exhibits potential for PET imaging of GnRH receptor expression.

Data Availability

All data included in this study are available upon request from the first author or corresponding author.

Conflicts of Interest

The authors declare that they have no conflicts of interest.

Authors' Contributions

KH, SH, HL, YH, LF, YR, YZ, YL, PS, and MW conducted the experiments and analyzed the data. KH, HW, and QW designed the experiments. KH wrote the manuscript. All authors have given approval to the final version of the manuscript. Shun Huang and Hongsheng Li contributed equally to this article.

Acknowledgments

This research was supported by grants from the National Natural Science Foundation of China (81701729 and 81501511), Scientific Research Foundation of Southern Medical University (C1034414 and C1051440), Outstanding Youths Development Scheme of Nanfang Hospital, Southern Medical University (2017J010), and President Foundation Project of Nanfang Hospital, Southern Medical University (2015C027).

Supplementary Materials

Some original data of NMR, MS, and HPLC for the PET tracer of [¹⁸F]FP-D-Lys⁶-GnRH are provided in the supplementary information file. Figure S1: ¹H and ¹³C-NMR spectra of 4-nitrophenyl-2-fluoropropionate (NFP). Figure S2: mass spectra of FP-D-Lys⁶-GnRH. Figure S3: semipreparative radio-high-performance liquid chromatography (radio-HPLC) of [¹⁸F]NFP. Figure S4: radio-HPLC of [¹⁸F]FP-D-Lys⁶-GnRH for in vitro stability. (*Supplementary Materials*)

References

- [1] A. V. Schally, A. Arimura, A. J. Kastin et al., "Gonadotropin-releasing hormone: one polypeptide regulates secretion of luteinizing and follicle-stimulating hormones," *Science*, vol. 173, no. 4001, pp. 1036–1038, 1971.
- [2] C. Gründker and G. Emons, "The role of gonadotropin-releasing hormone in cancer cell proliferation and metastasis," *Frontiers in Endocrinology*, vol. 8, pp. 1–10, 2017.
- [3] C. Leuschner and W. Hansel, "Targeting breast and prostate cancers through their hormone receptors1," *Biology of Reproduction*, vol. 73, no. 5, pp. 860–865, 2005.
- [4] I. Bjelobaba, S. S. Stojilkovic, and Z. Naor, "Editorial: gonadotropin-releasing hormone receptor signaling and functions," *Frontiers in Endocrinology*, vol. 9, pp. 10–12, 2018.
- [5] M. L. Dufau, "The luteinizing hormone receptor," *Annual Review of Physiology*, vol. 60, no. 1, pp. 461–496, 1998.
- [6] A. Nagy and A. V. Schally, "Targeting of cytotoxic luteinizing hormone-releasing hormone analogs to breast, ovarian, endometrial, and prostate cancers1," *Biology of Reproduction*, vol. 73, no. 5, pp. 851–859, 2005.
- [7] Å. Tieva, P. Stattin, P. Wikström, A. Bergh, and J.-E. Damber, "Gonadotropin-releasing hormone receptor expression in the human prostate," *The Prostate*, vol. 47, no. 4, pp. 276–284, 2001.
- [8] M. Fekete, A. Zalatnai, A. M. Comaru-schally, and A. V. Schally, "Membrane receptors for peptides in experimental and human pancreatic cancers," *Pancreas*, vol. 4, no. 5, pp. 521–528, 1989.
- [9] C. Gründker, P. Völker, F. Griesinger et al., "Antitumor effects of the cytotoxic luteinizing hormone-releasing hormone analog AN-152 on human endometrial and ovarian cancers xenografted into nude mice," *American Journal of Obstetrics and Gynecology*, vol. 187, no. 3, pp. 528–537, 2002.
- [10] T. M. Bateman, "Advantages and disadvantages of PET and SPECT in a busy clinical practice," *Journal of Nuclear Cardiology*, vol. 19, no. S1, pp. 3–11, 2012.
- [11] C. A. Flanagan, B. J. Fromme, J. S. Davidson, and R. P. Millar, "A high affinity gonadotropin-releasing hormone (GnRH) tracer, radioiodinated at position 6, facilitates analysis of mutant GnRH Receptors1," *Endocrinology*, vol. 139, no. 10, pp. 4115–4119, 1998.
- [12] H. Gali, T. J. Hoffman, G. L. Sieckman, N. K. Owen, K. V. Katti, and W. A. Volkert, "Synthesis, characterization, and labeling with ^{99m}Tc/¹⁸⁸Re of peptide conjugates containing a dithia-bisphosphine chelating agent," *Bioconjugate Chemistry*, vol. 12, no. 3, pp. 354–363, 2001.
- [13] Y. Barda, N. Cohen, V. Lev et al., "Backbone metal cyclization: novel ^{99m}Tc labeled GnRH analog as potential SPECT molecular imaging agent in cancer," *Nuclear Medicine and Biology*, vol. 31, no. 7, pp. 921–933, 2004.
- [14] M. Schottelius, S. Berger, T. Poethko, M. Schwaiger, and H.-J. Wester, "Development of Novel ⁶⁸Ga- and ¹⁸F-labeled GnRH-I analogues with high GnRHR-targeting efficiency," *Bioconjugate Chemistry*, vol. 19, no. 6, pp. 1256–1268, 2008.
- [15] A. R. Jalilian, S. Shanehsazzadeh, M. Akhlaghi et al., "Development of [¹¹¹In]-DTPA-buserelin for GnRH receptor studies," *Radiochim Acta*, vol. 98, pp. 113–119, 2010.
- [16] H. Guo, J. Lu, H. Hathaway, M. E. Royce, E. R. Prossnitz, and Y. Miao, "Synthesis and evaluation of novel gonadotropin-releasing hormone receptor-targeting peptides," *Bioconjugate Chemistry*, vol. 22, no. 8, pp. 1682–1689, 2011.
- [17] M. Zoghi, A. R. Jalilian, A. Niazi, F. Johari-daha, B. Alirezapour, and S. Ramezanpour, "Development of a ⁶⁸Ga-peptide tracer for PET GnRH1-imaging," *Annals of Nuclear Medicine*, vol. 30, no. 6, pp. 400–408, 2016.
- [18] J. Xu, C. Feng, and Y. Miao, "Evaluation of novel ¹¹¹In-labeled gonadotropin-releasing hormone peptides for human

- prostate cancer imaging,” *Bioorganic & Medicinal Chemistry Letters*, vol. 27, no. 20, pp. 4647–4651, 2017.
- [19] I. Lee, J. C. Paeng, S. J. Lee et al., “Comparison of diagnostic sensitivity and quantitative indices between ^{68}Ga -DOTATOC PET/CT and ^{111}In -pentetreotide SPECT/CT in neuroendocrine tumors: a preliminary report,” *Nuclear Medicine and Molecular Imaging*, vol. 49, no. 4, pp. 284–290, 2015.
- [20] M. J. Karten and J. E. Rivier, “Gonadotropin-releasing hormone analog design. Structure-function studies toward the development of agonists and antagonists: rationale and perspective,” *Endocrine Reviews*, vol. 7, no. 1, pp. 44–66, 1986.
- [21] T. Beckers, M. Bernd, B. Kutscher, R. Kühne, S. Hoffmann, and T. Reissmann, “Structure-function studies of linear and cyclized peptide antagonists of the GnRH receptor,” *Biochemical and Biophysical Research Communications*, vol. 289, no. 3, pp. 653–663, 2001.
- [22] S. Liu, H. Liu, G. Ren, R. H. Kimura, J. R. Cochran, and Z. Cheng, “PET imaging of integrin positive tumors using ^{18}F labeled knottin peptides,” *Theranostics*, vol. 1, pp. 403–412, 2011.
- [23] K.-Z. Hu, H. Wang, G. Tang et al., “Automated synthesis of symmetric integrin $\alpha\text{v}\beta\text{3}$ -targeted radiotracer [^{18}F]FP-PEG3- β -Glu-RGD2,” *Journal of Radioanalytical and Nuclear Chemistry*, vol. 299, no. 1, pp. 271–276, 2014.
- [24] M. Hachem, M. Tiberi, B. Ismail et al., “Characterization of ^{18}F -FPyKYNE-Losartan for imaging AT1 receptors,” *Journal of Nuclear Medicine*, vol. 57, no. 10, pp. 1612–1617, 2016.
- [25] Z. Feng, H. Wen, X. Ju et al., “Expression of hypothalamic-pituitary-gonadal axis-related hormone receptors in low-grade serous ovarian cancer (LGSC),” *Journal of Ovarian Research*, vol. 10, no. 1, pp. 1–8, 2017.
- [26] S. V. Liu, A. V. Schally, D. Hawes et al., “Expression of receptors for luteinizing hormone-releasing hormone (LH-RH) in prostate cancers following therapy with LH-RH agonists,” *Clinical Cancer Research*, vol. 16, no. 18, pp. 4675–4680, 2010.
- [27] W.-H. Yang, M. Wiczorck, M. C. Allen, and T. M. Nett, “Cytotoxic activity of gonadotropin-releasing hormone (GnRH)-pokeweed antiviral protein conjugates in cell lines expressing GnRH receptors,” *Endocrinology*, vol. 144, no. 4, pp. 1456–1463, 2003.
- [28] A. Schally and A. Nagy, “Cancer chemotherapy based on targeting of cytotoxic peptide conjugates to their receptors on tumors,” *European Journal of Endocrinology*, vol. 141, pp. 1–14, 1999.
- [29] S. C. Penchala, M. R. Miller, A. Pal et al., “A biomimetic approach for enhancing the in vivo half-life of peptides,” *Nature Chemical Biology*, vol. 11, no. 10, pp. 793–798, 2015.
- [30] N. V. Nukolova, H. S. Oberoi, Y. Zhao, V. P. Chekhonin, A. V. Kabanov, and T. K. Bronich, “LHRH-targeted nanogels as a delivery system for cisplatin to ovarian cancer,” *Molecular Pharmaceutics*, vol. 10, no. 10, pp. 3913–3921, 2013.
- [31] N. Eicke, A. R. Günthert, G. Emons, and C. Gründker, “GnRH-II agonist [d-Lys6]GnRH-II inhibits the EGF-induced mitogenic signal transduction in human endometrial and ovarian cancer cells,” *International Journal of Oncology*, vol. 29, pp. 1223–1229, 2006.
- [32] M. Letsch, A. V. Schally, K. Szepeshazi, G. Halmos, and A. Nagy, “Preclinical evaluation of targeted cytotoxic luteinizing hormone-releasing hormone analogue AN-152 in androgen-sensitive and insensitive prostate cancers,” *Clinical Cancer Research*, vol. 9, no. 12, pp. 4505–4513, 2003.
- [33] T. Karampelas, O. Argyros, N. Sayyad et al., “GnRH-gemcitabine conjugates for the treatment of androgen-independent prostate cancer: pharmacokinetic enhancements combined with targeted drug delivery,” *Bioconjugate Chemistry*, vol. 25, no. 4, pp. 813–823, 2014.
- [34] A. P. Kafka, T. Kleffmann, T. Rades, and A. McDowell, “Histidine residues in the peptide d-Lys6-GnRH: potential for copolymerization in polymeric nanoparticles,” *Molecular Pharmaceutics*, vol. 6, no. 5, pp. 1483–1491, 2009.
- [35] H. Chen, G. Niu, H. Wu, and X. Chen, “Clinical application of radiolabeled RGD peptides for PET imaging of integrin $\alpha\text{v}\beta\text{3}$,” *Theranostics*, vol. 6, no. 1, pp. 78–92, 2016.